Supplementary Information

Gain-of-function variants in *SYK* cause immune dysregulation and systemic inflammation in humans and mice

SUPPLEMENTARY NOTE

Extended Patient Phenotype:

Patient 1 (p.S550Y): This patient was a female of Chinese origin and born to non-consanguineous parents with a healthy brother. She presented with recurrent fever, whole body rash and non-bloody diarrhea at 2 weeks of age. Steroids and antibiotics were administrated but her condition did not improve. She was transferred to a tertiary hospital and found to have high WBC, elevated CRP, hypoalbuminemia and anemia. She required transfusion of albumin and red cells. Colonoscopy was performed at 2 months of age which showed perianal skin tags and many intestinal ulcers. Histopathological analysis revealed infiltration of chronic inflammatory cells. The patient was diagnosed with Crohn's disease. She also had pneumonia at that time. She was treated with mesalamine, corticosteroids, meropenem, and intravenous immunoglobulin. She went on to have recurrent infections. She experienced recurrent fever, intractable diarrhea and subsequent colorectal fistula. At the age of 17 months, her weight was only 5 kg (well below a z-score of -3) with severe malnutrition. She then received a wide spectrum of antibiotics, including sulperazone, metronidazole, linezolid and diflucan. She also required enteral nutritional support. When she was 26 months old and 7.2 kg, another GI endoscopy was performed and revealed perianal fistula, mucosal ulcers in rectum and colon, nodularity throughout the colon and hyperplastic lesions of the gastric antrum. Immunologic analyses showed normal numbers and function of T cells, B cells and NK cells. Serum immunoglobulin levels (IgM and IgG) were low (**Supplementary Table 1**). Colitis was a predominant feature in Patient 1 who was also a heterozygous carrier for a missense p.R124Q variant in the *IL10* gene [1] (CADD score of 22.9; ExAC [2] minor allelic frequency of 0.00008) a known biallelic cause of monogenic IBD [3] and could potentiate the colonic disease that was observed in this patient. Despite ongoing aggressive therapy, including treatment with antibiotics, steroids and thalidomide, she unfortunately died before she was 3 years old.

Patient 2 (p.S550F): This patient is a female of Ashkenazi Jewish descent with an autoinflammatory condition of unknown etiology and pits behind her ears. She was born at term after an uneventful pregnancy and delivery. Her parents are not consanguineous. At 2 weeks of age, she developed vomiting and then diarrhea, fever and a nonspecific macular-pustular rash. Endoscopy at about 1 month of age showed scalloping with ulceration and erythema in the duodenum. Histology showed mild chronic lymphocyte plasma cell gastritis in sigmoid colon and focal ulcers in cecum with associated chronic inflammation. A skin biopsy showed small vessel mixed but predominantly lymphocytic vasculitis. She had persistently elevated inflammatory markers that improved but did not resolve with anakinra (interleukin 1 receptor antagonist) and prednisone (initial dose of 2 mg/kg/day). She was transitioned to tacrolimus and underwent a gradual wean of her prednisone over the ensuing months. Her symptoms and inflammatory markers (especially CRP) were controlled on tacrolimus although her rash waxed and waned throughout (**Supplementary Table 2**). She required multiple increases in her prednisone and/or tacrolimus doses between one and six months of age due to rising inflammatory markers and/or symptoms. At seven months of age, she was treated with two doses rituximab (750 mg/m^2, two weeks apart). B lymphocyte depletion was confirmed 1.5 months later. Her prednisone was weaned and discontinued by one year of age. At the same time, her B lymphocytes had reconstituted, and she remained well. Another single dose of rituximab was given at about 13 months of age, with confirmed B lymphocyte depletion again. Approximately two months later, she developed a recurrence of disease with fever, diarrhea, rash and elevated inflammatory markers and rituximab was stopped. Corticosteroids were restarted and both symptoms and inflammatory markers improved. However, as her steroids were being tapered, she developed right tibiotalar and subtalar arthritis as well as tenosynovitis of the peroneal tendons, which were treated with corticosteroid injections. Repeat chest x-rays showed evidence of bronchiectasis. Repeat colonoscopy showed evidence of chronic right-sided colitis and treatment with vedolizumab was initiated.

Patient 3 (p.S550F): This is Patient 2's father who is of Ashkenazi Jewish descent and he also has similar pits behind his ears. He has a history of a severe illness beginning at 2 weeks of life with oral ulcers, fever and rash treated with antibiotics then progressing prolonged diarrheal illness and anemia leading to hypernatremia and hypoalbuminemia requiring parenteral nutrition for weeks, and prolonged hospitalization for months. He was labelled as having an immunodeficiency of unknown etiology at the time with low T lymphocyte populations and low lymphocyte mitogen stimulation and low IgG levels. As a toddler, he was found to have a cholesteatoma (pathology confirmed) at two years of age with recurrence and re-removal at four and seven years of age. For most of his adult life Patient 2's father has had symptoms attributed to irritable bowel syndrome. He had an endoscopy at 33 years old that showed intraepithelial lymphocytosis in the duodenum. He has had debilitating joint swelling in his ankles and elevated CRP between 18-31 mg/L (**Supplementary Table 3**).

Immunophenotyping data shows B cell abnormalities of P2 and her father P3 but not the unaffected mother. $CD4^+$ T cells also demonstrated increased frequencies of $CD4^+CD25^-$ $CD45RA^-CCR6^+RORgt^+$ cells, that expressed elevated IL-22 and IL-17A compared to healthy controls (**Supplementary Table 4** and data not shown).

Patient 4 (p.P342T): This is a female patient of Hungarian origin born to non-consanguineous parents. The patient suffered from recurrent abscess formation on the hands and feet between ages 12 to 20 years old, which required regular surgical intervention. The patient was first hospitalized at age 20 after she presented with abdominal pain, anorexia, and lymphadenopathy. Lymph node biopsy revealed reactive follicular hyperplasia. She was found to have hypogammaglobinemia with a decrease in IgG, IgM, and IgA (**Supplementary Table 5**). Treatment with intravenous immunoglobulins (IVIG) led to the cessation of cutaneous infections. At age 26 the patient presented at the hospital with severe thoracic pain, non-radicular hemiparesthesia of the left side and paresis of the left lower limb. CT scan revealed a spinal lesion (**Extended Data Fig. 2b**), multiple enlarged lymph nodes, and two 2.5 cm nodular lesions in the lower lobe of both lungs. Histologic examination of the spinal cord lesion revealed granulomatous lesions containing giant cells. These inflammatory findings responded well to high dose steroids. The spinal lesion recurred approximately annually. Maintenance immunosuppressive therapy began at age 26 and consisted of cyclosporine A 200 mg/day and was later switched to Azathioprine 50 mg/day. At age 27, the patient presented with severe diarrhea, abdominal pain, and drastic weight loss over the course of several months. Gastroscopy and colonoscopy revealed greyish-white plaques in the stomach. Histological examination of the gut showed lymphocytic gastritis and colitis with increased intraepithelial lymphocytes and lymphoid aggregates. High dose steroid therapy induced a gradual regression of the gastrointestinal symptoms. Nevertheless, spinal inflammation reappeared at age 29 and this time was resistance to steroids and featured morning stiffness in the small joints of the left upper extremity. After prolonged treatment with insufficient response, the patient was treated with rituximab and the inflammation-associated pain and the majority of symptoms responded promptly; however, there is now loss of response. However, residual inflammatory activity was still detectable in the spinal cord at age 31. No elevation of CRP was observed during disease flares in this patient.

Patient 5 (p.M450I): This patient is a female who presented at 34 years with a history of recurrent infections including bronchitis, pneumonia, salmonellosis, *Helicobacter pylori* and herpes zoster infection. She had hypogammaglobinaemia with an IgG of 3.08g/L, IgA <0.22g/L and IgM <0.17g/L, splenomegaly, lymphadenopathy and inflammatory CNS lesions. Lymphocyte immunophenotyping showed low B cell numbers (63 cells/μL) and reduced NK cell numbers (62 cells/μL). Total $CD3^+$ T cell numbers were within the normal range (1330 cells/μL), while naïve $CD3^+CD4^+$ T cells (3.70 %) and $CD3^+CD8^+$ T cells (5.53 %) were reduced indicating memory expansion and immune activation. Nine years later she developed diarrhea and weight loss. Colonoscopy showed villus atrophy, mild mucosal edema, capillary ectasia, low grade chronic mucosal inflammation and low grade proctitis. Fifteen years after initial presentation, the patient was diagnosed with diffuse non-GC large B cell lymphoma.

Patient 6 (p.A353T): This is a male with a lifelong history of recurrent acute otitis media who presented at 44 years of age with a large thigh abscess and osteomyelitis caused by *streptococcus* spp. He had lymphadenopathy, splenomegaly and hypogammaglobulinemia with an IgG of 1.3g/L, IgA <0.30g/L and IgM <0.22g/L. Lymphocyte surface markers showed low B cell numbers (42 cells/μl) and reduced NK cell numbers (47 cells/μL) but normal T cell numbers (1114 cells/μL). $CD27^{-}IgM^{+}IgD^{+}$ (naïve) B cells 92%, $CD27^{+}$ $IgM^{+}IgD^{+}$ (memory) B cells 6% and $CD27^{+}$ IgM^{-} IgD^{-} class switched memory B cells 0%. CT scans revealed multiple lung nodules and splenomegaly (25cm diameter) and multiple enlarged intra-abdominal lymph nodes were noted. Diagnosis of CVID was made and immunoglobulin replacement therapy was started. One year later, he developed granulomatous cervical lymphadenopathy. Two years after initial presentation he developed stiffness and pain in his hands, wrists and shoulder joints, with x-rays showing mild degenerative changes. Shortly thereafter, he presented with bloody diarrhoea due to *Campylobacter* gastroenteritis that resolved with ciprofloxacin treatment. Then his liver enzymes became abnormal (ALT 54, alkaline phosphatase 133, GGT 173). A liver biopsy revealed granulomatous hepatitis, which has persisted for the subsequent 7 years. Six years after initial presentation, he experienced diarrhea and weight loss. Endoscopy showed gastritis and mild to moderate active colitis with apoptosis, infiltrating eosinophils and scattered lymphocytes. No granulomas were seen. SeHCAT scan showed significant bile salt malabsorption now successfully treated with colesevelam. CT showed osteomalacia with partial collapse of L5 and possible sacral fracture attributed to metabolic bone disease. This was managed with bisphosphonate. The patient has had persistent lymphadenopathy throughout the last 9 years. Seven years after initial presentation, the patient was diagnosed with diffuse large B cell non Hodgkin's lymphoma stage 4B and treated with 6 cycles of CHOP-R chemotherapy. He remains in remission and is currently not on any treatment.

Supplementary Methods

DNA purification and sanger sequencing from buccal swaps – Patient 5 and Patient 6: Briefly, genomic DNA was purified from buccal swab samples according to the QIAamp® DNA Mini Kit (Qiagen) standard protocol. DNA concentration was read using a NanoDrop spectrophotometer (ThermoFisher). DNA was amplified by PCR (35 cycles, 66°C annealing temperature) using the Phusion High-Fidelity Taq polymerase (Thermos-Fisher):

Patient 5 (p.M450I) Oligos:
Fw-5' ACTCTGTGGCAGGTATTTCCG
Rw-5' AATAAAGGAAGGCACAGGAGGG

Patient 6 (p.A353T) Oligos:
Fw-5' CACATCTAGTGGCAGGCAGC
Rw-5' AGGCTGGTGGAACATAGCAACT

Generation of SYK (S544Y) mouse model – sgRNA and ssODN sequences:

Syk sgRNA (5'-3'):
TCCAGACGTCACTCTTAC

Syk (C>A) ssODN (5'-3'):
CCAGACCCACGGGAAGTGGCCCGTGAAGTGGTACGCCCCCGAATGCATCAACTACT
ACAAGTTCTACAGCAAGAGTGACGTCTGGAGCTTCGGAGTCCTGATGTGGGAAGCG
TTCTCCTA

Analysis of wild-type and SYK^{S544Y} cytokine expression – RT-qPCR primers sequences:

Ifng-F:
AGGAACTGGCAAAAGGATGGT
Ifng-R:
TCATTGAATGCTTGGCGCTG

Il4-F:
TCACTGACGGCACAGAGCTA
Il4-R:
CTGTGGTGTTCTTCGTTGCTG

Il17a-F:
GGACTCTCCACCGCAATGA
Il17a-R: GTTTGCTGAGAAACGTGGGG

Il17f-F:
GCCATTCTGAGGGAGGTAGC
Il17f-R:
GGGGTCTCGAGTGATGTTGT

Csf2-F:
TCACTGGCCCCATGTATAGC
Csf2-R:
CTTCATTCAACGTGACAGGCA

References

1. Glocker, E.O. *et al.* Infant colitis--it's in the genes. *Lancet* **376**, 1272 (2010).
2. Karczewski, K.J. *et al.* The ExAC browser: displaying reference data information from over 60 000 exomes. *Nucleic Acids Res* **45**, D840-D845 (2017).
3. Uhlig, H.H. *et al.* The diagnostic approach to monogenic very early onset inflammatory bowel disease. *Gastroenterology* **147**, 990-1007 e3 (2014).

Supplementary List of Genomics England Research Consortium Members

John C. Ambrose[1]; Prabhu Arumugam[1]; Emma L. Baple[1]; Marta Bleda[1]; Freya Boardman-Pretty[1,2]; Jeanne M. Boissiere[1]; Christopher R. Boustred[1]; Helen Brittain[1]; Mark J. Caulfield[1,2]; Georgia C. Chan[1]; Clare E. H. Craig[1]; Louise C. Daugherty[1]; Anna de Burca[1]; Andrew Devereau[1]; Greg Elgar[1,2]; Rebecca E. Foulger[1]; Tom Fowler[1]; Pedro Furió-Tarí[1]; Adam Giess[1]; Joanne M. Hackett[1]; Dina Halai[1]; Angela Hamblin[1]; Shirley Henderson[1,2]; James E. Holman[1]; Tim J. P. Hubbard[1]; Kristina Ibáñez[1,2]; Rob Jackson[1]; Louise J. Jones[1,2]; Dalia Kasperaviciute[1,2]; Melis Kayikci[1]; Athanasios Kousathanas[1]; Lea Lahnstein[1]; Kay Lawson[1]; Sarah E. A. Leigh[1]; Ivonne U. S. Leong[1] ; Javier F. Lopez[1]; Fiona Maleady-Crowe[1]; JoanneMason[1]; Ellen M. McDonagh[1,2]; Loukas Moutsianas[1,2]; Michael Mueller[1,2]; Nirupa Murugaesu[1]; Anna C. Need[1,2]; Peter O'Donovan[1]; Chris A. Odhams[1]; Andrea Orioli[1]; Christine Patch[1,2]; Mariana Buongermino Pereira[1]; Daniel Perez-Gil[1]; Dimitris Polychronopoulos[1]; John Pullinger[1]; Tahrima Rahim[1]; Augusto Rendon[1]; Pablo Riesgo-Ferreiro[1]; Tim Rogers[1]; Mina Ryten[1]; Kevin Savage[1]; Kushmita Sawant[1]; Richard H. Scott[1]; Afshan Siddiq[1]; Alexander Sieghart[1]; Damian Smedley[1,2]; Katherine R. Smith[1,2]; Samuel C. Smith[1]; Alona Sosinsky[1,2]; William Spooner[1]; Helen E. Stevens[1]; Alexander Stuckey[1]; Razvan Sultana[1]; Mélanie Tanguy[1]; Ellen R. A. Thomas[1,2]; Simon R. Thompson[1]; Carolyn Tregidgo[1]; Arianna Tucci[1,2]; Emma Walsh[1]; Sarah A. Watters[1]; Matthew J. Welland[1]; Eleanor Williams[1]; Katarzyna Witkowska[1,2]; Suzanne M. Wood[1,2]; Magdalena Zarowiecki[1].

1. Genomics England, London, UK
2. William Harvey Research Institute, Queen Mary University of London, London, EC1M 6BQ, UK.

SUPPLEMENTARY FIGURES

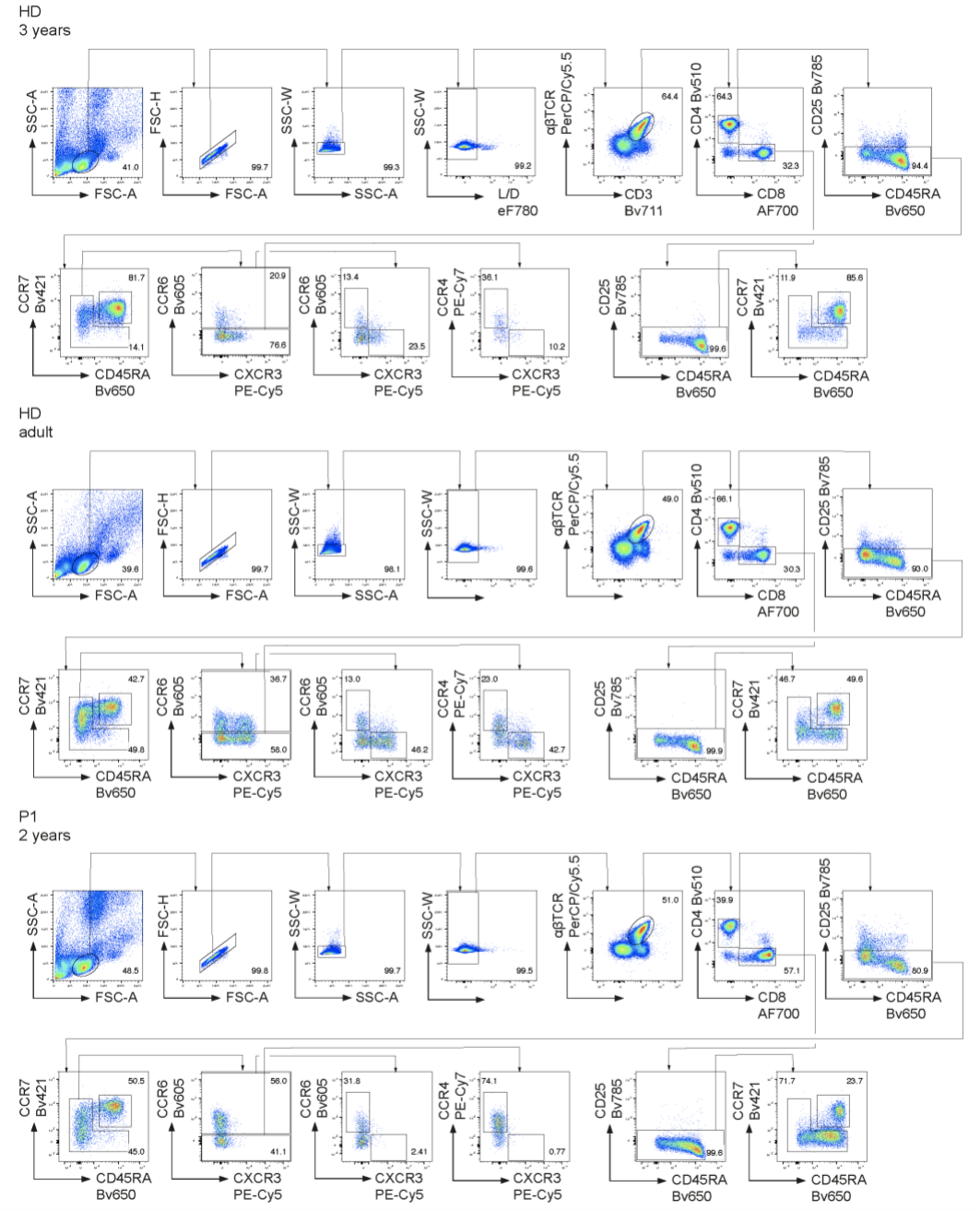

Supplementary Figure 1: Analysis of T cell phenotype and function by flow cytometry – Gating strategy – Surface marker expression. Representative gating strategy of flow cytometry data obtained from unstimulated surface stained PBMC samples. Shown are PBMC samples from a healthy donor at 3 years of age, an adult healthy donor and PBMC from P1 at 2 years of age.

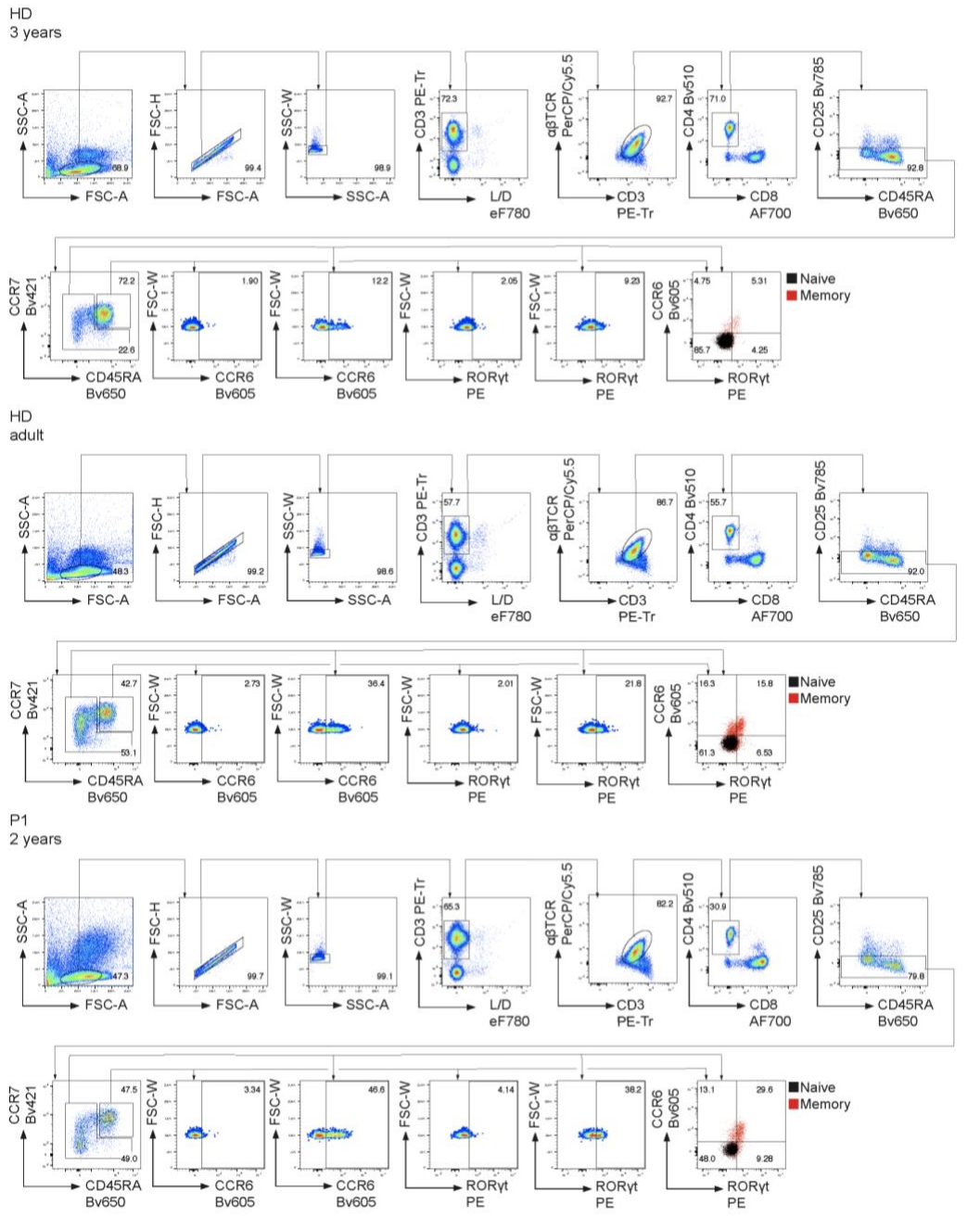

Supplementary Figure 2: Analysis of T cell phenotype and function by flow cytometry – Gating strategy – Combined surface marker and transcription factor expression. Representative gating strategy of flow cytometry data obtained from unstimulated combined surface and intracellularly stained PBMC samples. Shown are PBMC samples from a healthy donor at 3 years of age, an adult healthy donor and PBMC from P1 at 2 years of age.

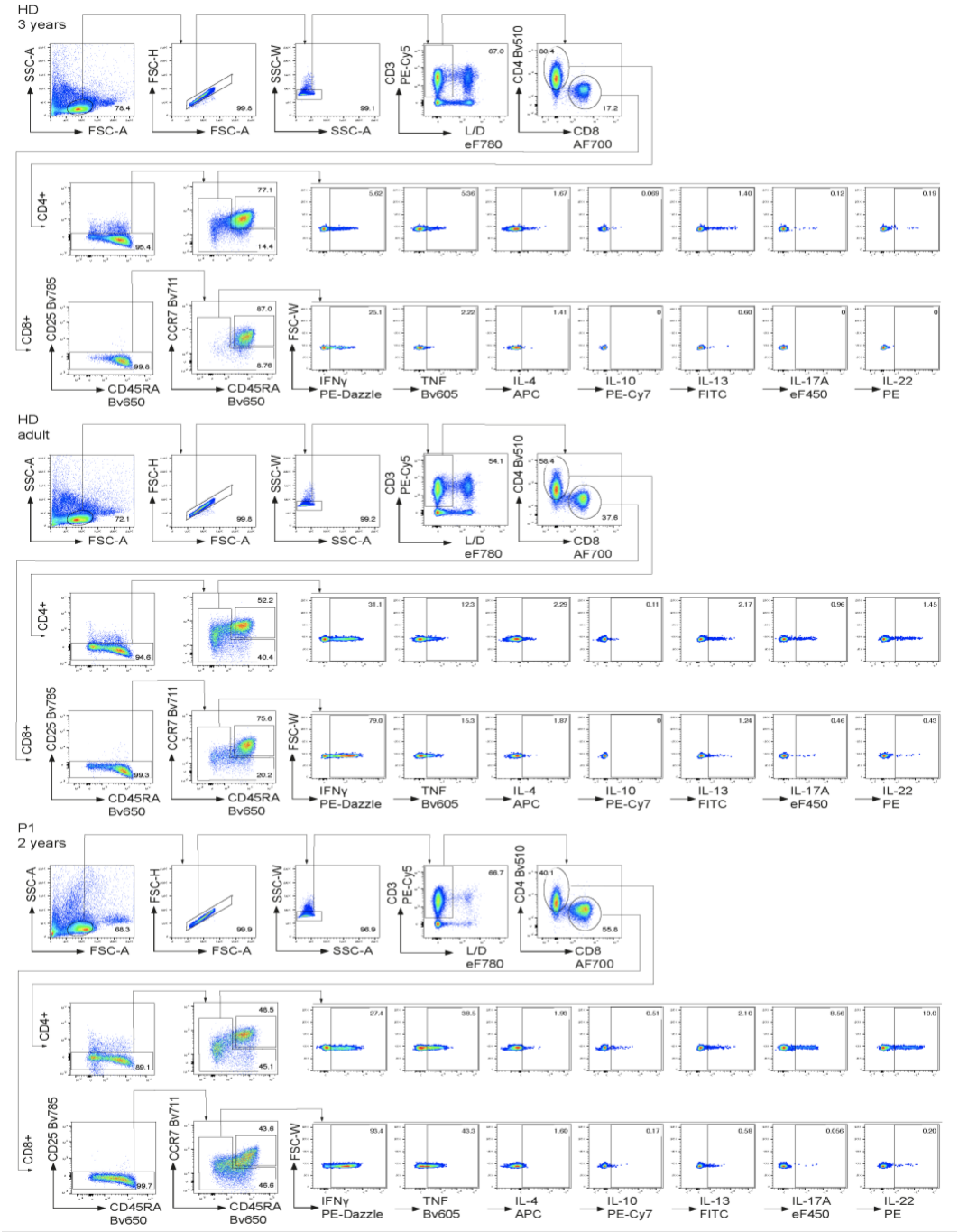

Supplementary Figure 3: Analysis of T cell phenotype and function by flow cytometry – Gating strategy – Intracellular cytokine staining. Representative gating strategy on flow cytometry data obtained from 5 hours PMA/ionomycin stimulated combined surface and intracellularly stained PBMC samples. Shown are PBMC samples from a healthy donor at 3 years of age, an adult healthy donor and PBMC from P1 at 2 years of age.

```
hSYK_TYR_KD_371-626      TLEDKELGSGNFGTVKKGYYQMKKVVKTVAVKILKNEANDPALKDELLAEANVMQQLDNP
mSyk_TYR_KD_365-620      TLEDNELGSGNFGTVKKGYYQMKKVVKTVAVKILKNEANDPALKDELLAEANVMQQLDNP
                         ****:************************************************

hSYK_TYR_KD_371-626      YIVRMIGICEAESWMLVMEMAELGPLNKYLQQNRHVKDKNIIELVHQVSMGMKYLEESNF
mSyk_TYR_KD_365-620      YIVRMIGICEAESWMLVMEMAELGPLNKYLQQNRHIKDKNIIELVHQVSMGMKYLEESNF
                         ***********************************:************************

hSYK_TYR_KD_371-626      VHRDLAARNVLLVTQHYAKISDFGLSKALRADENYYKAQTHGKWPVKWYAPECINYYKFS
mSyk_TYR_KD_365-620      VHRDLAARNVLLVTQHYAKISDFGLSKALRADENYYKAQTHGKWPVKWYAPECINYYKFS
                         ************************************************************

hSYK_TYR_KD_371-626      SKSDVWSFGVLMWEAFSYGQKPYRGMKGSEVTAMLEKGERMGCPAGCPREMYDLMNLCWT
mSyk_TYR_KD_365-620      SKSDVWSFGVLMWEAFSYGQKPYRGMKGSEVTAMLEKGERMGCPAGCPREMYDLMNLCWT
                         ************************************************************

hSYK_TYR_KD_371-626      YDVENRPGFAAVELRL
mSyk_TYR_KD_365-620      YDVENRPGFTAVELRL
                         *********:******
```

Supplementary Figure 4: Amino acid alignment of the tyrosine kinase domains (KD) of human (h) SYK and mouse (m) SYK highlighting the conservation of SYK S550 and SYK S544 residues. Highly conserved activation loop residues are under-lined and activation loop phospho-regulatory sites are in bold.

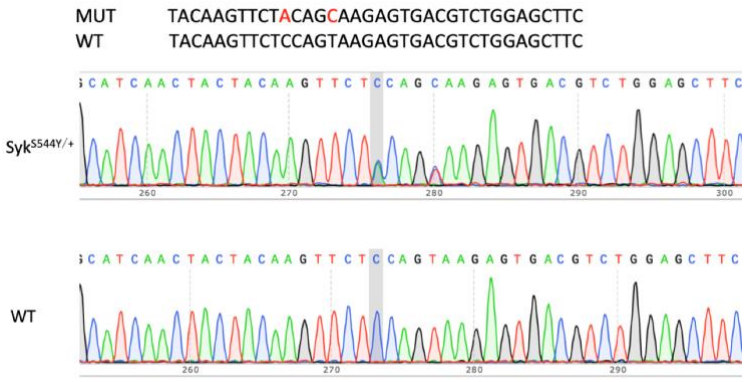

Supplementary Figure 5: Sanger sequencing validation of wild-type and heterozygous SYK^{S544Y} mice**.**

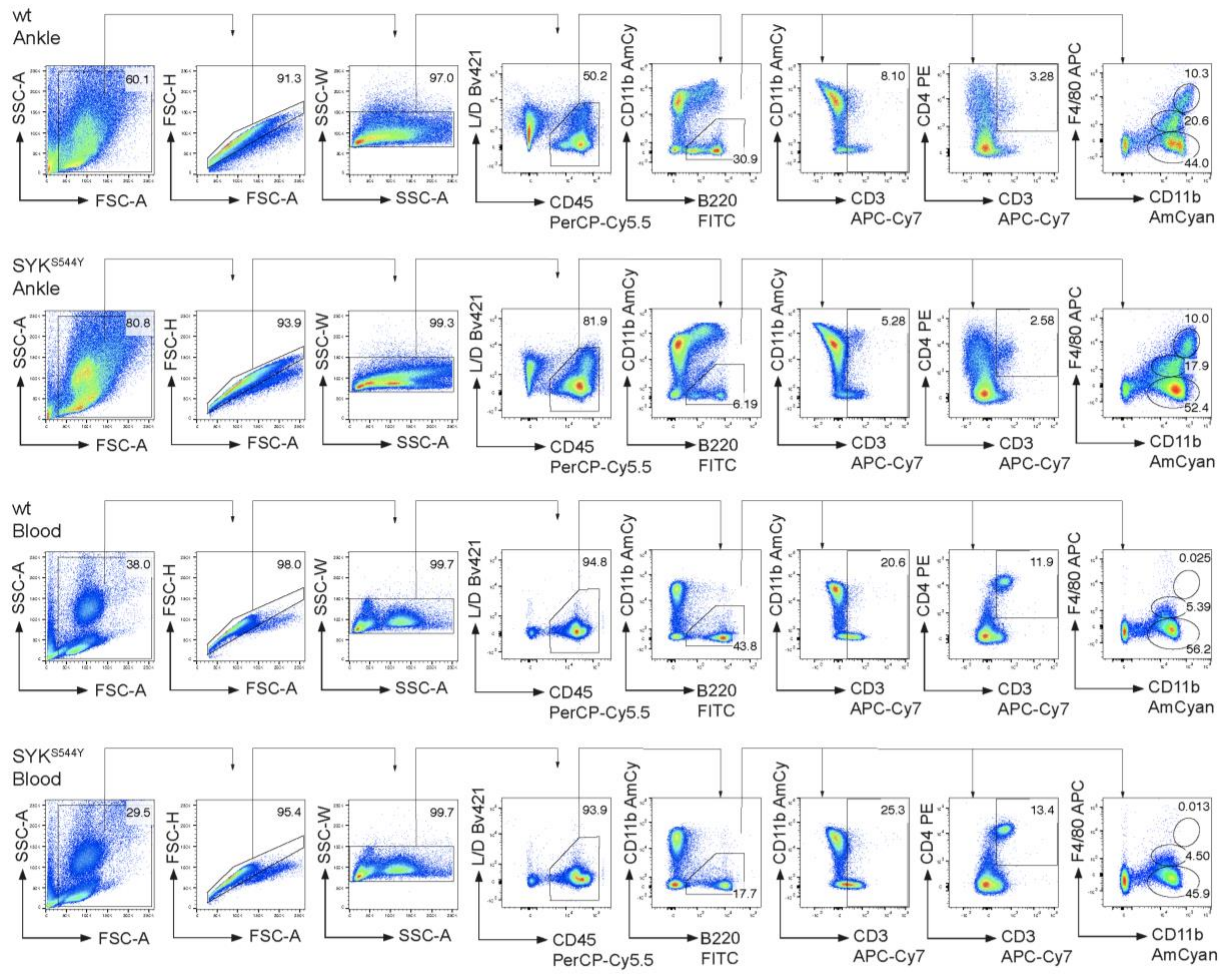

Supplementary Figure 6: Analysis of immune cell populations frequencies in wild-type and CRISPR-Cas9-knock-in SYK^{S544Y} mice – flow cytometry gating strategy

Gating of B220^{+} B cells, CD3^{+} T cells, CD4^{+} T cells, CD11b^{+}F4/80$^{–}$ mononuclear phagocytes, CD11b^{+}F4/80^{int} mononuclear phagocytes and CD11b^{+}F4/80^{+} macrophages (Mϕ) in ankles and blood of wild-type and SYK ^{S544Y} mice at the age of 3 months.

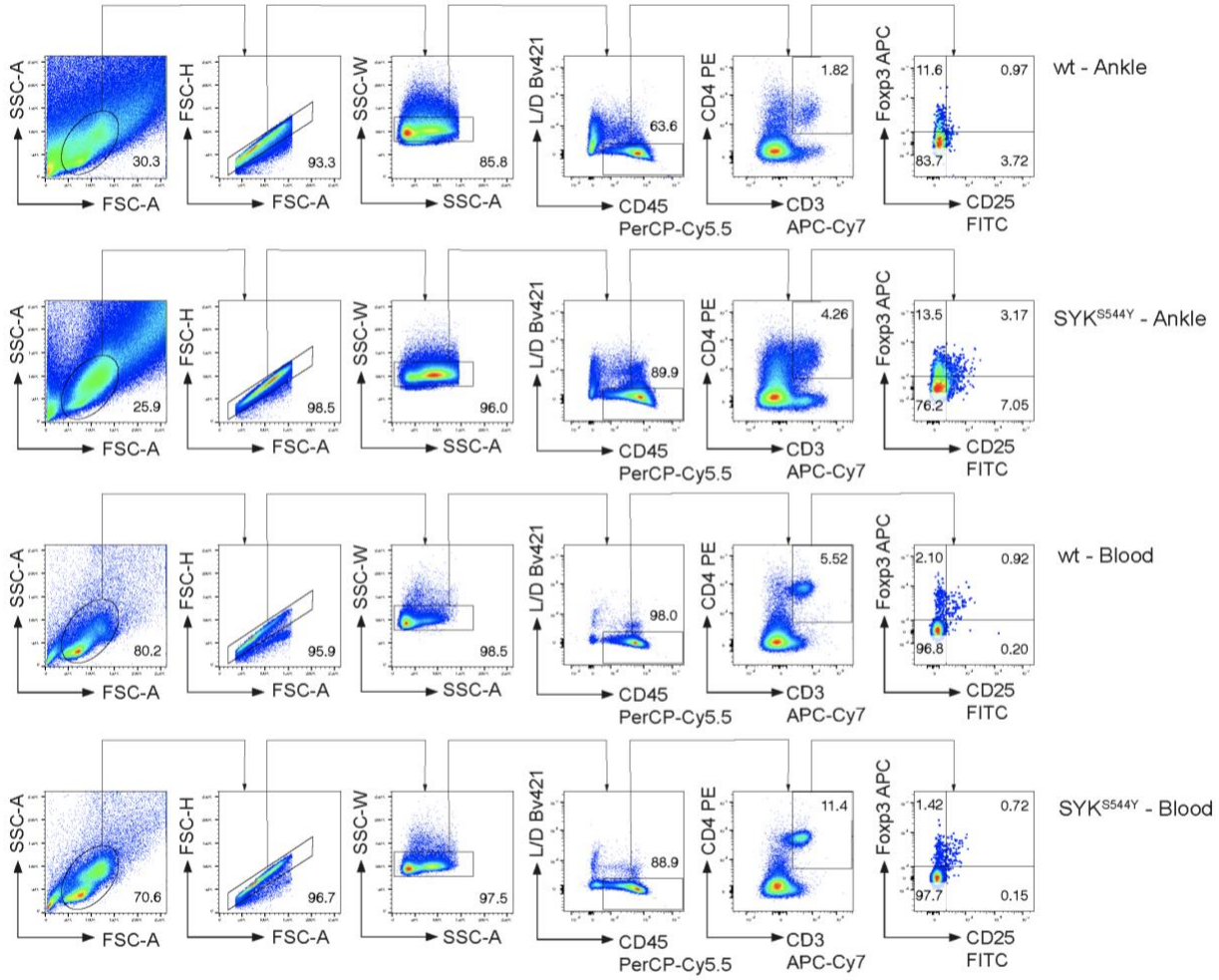

Supplementary Figure 7: Analysis of immune cell populations frequencies in wild-type and CRISPR-Cas9-knock-in SYK^{S544Y} mice – flow cytometry gating strategy

Representative gating of Foxp3^{+}CD25^{+} regulatory T cells (Treg) in ankles and blood of 3 months old wild-type and SYK^{S544Y} mice.